15TH IEA HEAT PUMP CONFERENCE
MAY 26–29, 2026 | HOFBURG VIENNA 2026
DECARBONISATION THROUGH INNOVATION

"Hydrogen based refrigeration process using an electro-chemical compressor"

Raimund Almbauer[a], Michael Lang[a], Lukas Dür[a], Jan Kummer[a], Kevin Wimmer[a], Michael Richter[b], Alexander Trattner[b]

[a]ITnA, University of Technology, Graz, Inffeldgasse 25b, A-8010 Graz, Austria
[b]HyCentA, Graz, Inffeldgasse 15, A-8010 Graz, Austria

Abstract

The evaporation of liquids (e.g. water) in the air is a well-known cooling method. This effect can be used in a hermetically sealed cycle in which a carrier gas transports vaporous refrigerant from an evaporation point via an internal heat exchanger to a condensation point. The evaporative heat exchanger absorbs heat from the cold room and transfers it to the surface wetted with liquid refrigerant, which evaporates at a low temperature. The carrier gas saturated with vaporized refrigerant is then heated in the internal counterflow heat exchanger to close to condensation temperature. In the condensation heat exchanger, the carrier gas is removed from the gas mixture, causing the partial pressure of the refrigerant to rise to the condensation pressure at the high temperature present. As a result, the refrigerant begins to condense, releasing the heat into the environment via the heat exchanger. To do this, the carrier gas must be effectively separated from the refrigerant after the condenser and recompressed to a higher pressure. The liquid refrigerant and the compressed carrier gas are finally cooled in the internal heat exchanger and fed back to the evaporative heat exchanger. The refrigeration process described here uses the working pair hydrogen and R600a as carrier gas and refrigerant respectively. An electrochemical H_2 membrane compressor is proposed for separation and compression. The advantage of this compressor is that it operates with absolutely no vibrations or noise emissions. This system is therefore suitable for use as a so-called "hotel refrigerator" in bedrooms or other acoustically sensitive areas. It achieves significantly better performance figures than the absorption-diffusion refrigerators currently used for this purpose.
This paper describes the underlying calculation model and uses it to derive the thermodynamic relationships for different operating conditions. The results are used for a basic design of the components. In particular, the design of the H_2 compressor is discussed and current data from research on achievable mass flows, pressures, pressure differences, separation efficiencies and efficiency as well as cooling capacity, temperatures and coefficient of performance of the cooling unit are described.

Keywords: Hydrogen-Isobutane refrigeration cycle, H2-compressor, minibar refrigerator

1. Introduction

Cooling fresh food, beverages and other perishable goods at temperatures above freezing point is an important factor in maintaining their quality and thus reducing waste. The associated energy consumption depends on the prevailing internal and ambient temperature levels, the type of appliance and the required cooling capacity. The temperature range for the system considered here extends from 4°C to approx. 18°C for the interior and 10°C to 43°C in the environment, whereby only exemplary boundary conditions are to be considered here. The hotel or minibar refrigerator with low cooling capacity represents the application that serves as the basis for the following explanations. One of the key drivers of the minbar refrigerator market is the increasing emphasis on health and wellness, as more guests prefer to store fresh food and beverages in their rooms. This demand is further intensified by increasing hotel tourism. Minibar refrigerators are a growing

application with a Compound Annual Growth Rate (CAGR) of approximately 9% between 2024 and 2033. The market size for hotel refrigerators has reached $1.2 billion by 2024 [1], with an estimated average price of $300, resulting in a volume of 4 million per annum.

Minibar refrigerators are usually operated with diffusion absorption refrigeration systems (DAR), which are powered purely by heat supply. In the case of an indirectly thermally heated diffusion absorption refrigeration machine, they can achieve a maximum coefficient of performance of 0.4 [2]. In normal operation, the coefficient of performance (COP) is less than half of that, at a maximum of 0.2 [3], [4]. However, it should be noted here that thermal energy for driving the DAR can also be supplied at temperatures just above 100°C, meaning that the exergy content is much smaller than 100%. Thermoelectric refrigerators can achieve COP values of up to 0.67 [5]. The combination of DAR with natural convection heat exchangers is another reason for their poor efficiency. In comparison, conventional vapor compression refrigeration systems with hermetic piston compressors and ventilated heat exchangers achieve coefficients of performance well above 2.0.

If the proposed cooling system with a COP of 1.2 for a standby cooling capacity of approx. 20 W halves energy consumption compared to DAR systems or thermoelectric systems, then savings of approximately 40 kWh/a per device can be expected. For the new devices alone, this results in a theoretical saving of 160 GWh.

The annual energy consumption of highly efficient minibar refrigerators is approximately 80 to 100 kWh/year with a cooling capacity of approximately 20 to 40 liters. The energy efficiency class is typically F. The EU's EPREL database [6] lists low-noise minibar refrigerators with higher energy efficiency classes (D). However, these values are listed only for two appliances with very small interior volumes of 19 liters and 25 liters, respectively, which suggests that the appliances contain sophisticated insulation. Nevertheless, the annual consumption of these top-rated appliances is 56 and 75 kWh, respectively. The consumption value of 75 kWh/year is only slightly lower than 88 kWh of the best freestanding combination appliances with dimensions of 60 x 60 x 200 cm, approx. 250 liters of cooling space and approx. 125 liters of freezer space [6]. The reason why DAR refrigerators are still widely used in this application is because they produce virtually no noise.

Another heat pump system that works with an electrochemical cell is the chemical looping heat pump process (CLHP). This type of heat pump is discussed in several publications [7], [8] and represents a fundamentally different system compared to the proposed system. In our proposed system, the two media H_2 and R600a remain chemically unchanged, only their mass composition is changed by the H_2 compressor. In contrast, in the CLHP, the chemical composition of the working medium, which usually consists of two components, is changed. The chemical conversion takes place through the operation of an electrochemical PEM cell, which removes or adds hydrogen atoms to the molecules. This results in different thermophysical properties before and after the chemical change, which can finally be used to transport heat. The CLHP system is an indirect chemical heat pump that utilizes the possibility of condensation after a chemical reaction to allow the working fluid's pressure increase to take place in the liquid phase. This reduces the power consumption for driving the heat pump system. In [9], a large number of working media were investigated as mixtures of two components. For the temperature range between 4°C and 45°C, which is relevant for the application of cooling appliances, high theoretical COPs are obtained eg. of 2 to 6.5. In [9], a large number of working media were investigated as mixtures of two components with also high potential COPs. Nevertheless, further work is needed on the materials, processes, and control systems for application in minibar refrigerators. Ultimately, the costs will also determine whether a market launch is possible.

The cooling process proposed here is also intended for use in a device with low maximum cooling capacity (approx. 50 W), moderate dimensions (approx. 40 x 40 x 50 cm; D x W x H) and no or minimal noise emission. However, the COP should be increased compared to the DAR system. The following paper presents a cooling process based on the principle of refrigerant evaporation which is explained in the following section. This is followed by a description of the system, the components and their arrangement in a fictitious minibar refrigerator. The following section describes the thermodynamic calculation with the underlying equations, boundary conditions, thermophysical properties [10] and the solution algorithm for a stationary case. After selecting typical boundary conditions, the results for the variation of different parameters are presented. An important part of the work involves describing the components of the refrigeration unit, in particular the H_2 compressor. The discussion of the results of the thermodynamic calculations is supplemented by considerations regarding feasibility.

2. System description: Evaporative cooling system

The evaporation or condensation of refrigerant in the presence of a second inert gas is already used in the DAR to generate a cooling process. In the proposed process, the inert gas hydrogen (H_2) transports vapor-

phase refrigerant (R600a) from an evaporation site to a condensation site via an internal heat exchanger in a hermetically sealed cycle. The evaporation heat exchanger absorbs heat from the cold room and transfers it to the surface wetted with liquid refrigerant, which evaporates at low temperatures. This cooling process is obviously based on the desiccant cooling cycle [11], but uses the working pair R600a and H_2 instead of water and air. The carrier gas saturated with vapor-phase refrigerant is then heated in the internal counterflow heat exchanger to near the condensation temperature. In the condensation heat exchanger, the carrier gas is removed from the gas mixture, causing the partial pressure of the refrigerant to rise to the condensation pressure at the prevailing high temperature. This causes the refrigerant to begin condensing, releasing heat to the environment via the heat exchanger. To do this, the carrier gas must be effectively separated from the refrigerant after the condenser and compressed again to a higher pressure. The liquid refrigerant and the compressed carrier gas are finally cooled in the internal heat exchanger and fed back to the evaporation heat exchanger. An electrochemical H_2 membrane compressor is proposed for separation and compression.

Fig. 1 shows the sketch of the cooling process with the components compressor, evaporator, internal heat exchanger (IHX) and condenser, and the direction of flow. It gives also an idea of the layered structure of the refrigeration system which forms vertical plates with a typical thickness of 5 cm.

For the calculation, it is assumed that the two media do not form a chemical compound but behave like pure substances. The two partial pressures add up to the total pressure, which is constant throughout the entire system except for flow pressure losses. The temperature of the two media at one location is the same. The tightness of the system is a prerequisite, of course. The internal heat exchanger is assumed to be adiabatic with respect to the environment. The exchanged heat output is calculated via the First Law of Thermodynamics for the individual heat exchangers using a control volume approach that guarantees compliance with the conservation laws and thermophysical properties. The size estimation of the heat exchanger components is based on realistic values for heat transfer from the VDI Wärme Atlas [12]. A saturated state for R600a is assumed at the outlet of the evaporator.

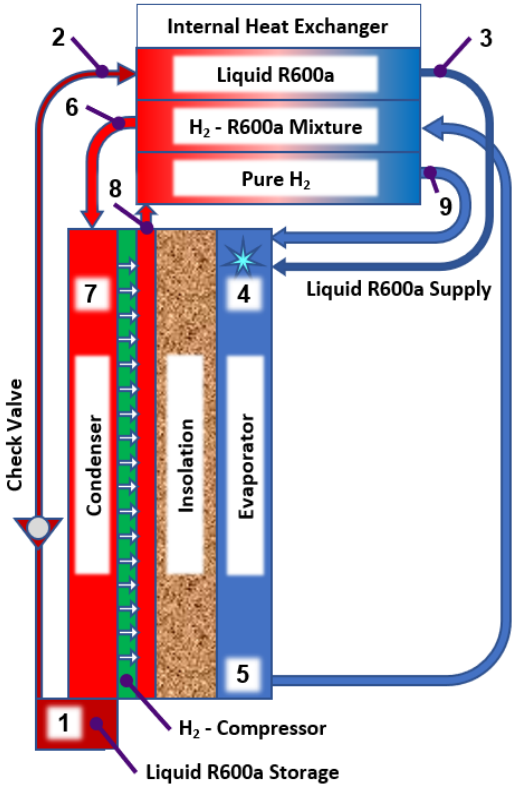

Figure 1. Sketch of the evaporative cooling system

The design of the H_2 membrane compressor is based on experimental results and literature studies conducted at HyCentA. The compressor is calculated using an isentropic change of state for the resulting pressures before and after the membrane, assuming that the membrane perfectly separates the two gases. An electrical efficiency of 0.9 is also taken into account when calculating the electrical power. A value of 1.0 bar is assumed for the pressure loss due to the mass flow of 0,1 g/s of H_2 through the heat exchanger channels and pipes, which ultimately also determines the flow cross-sections in the system. In order to assess the pressure losses values from the Moody diagram are used with estimates of the Reynolds numbers and the roughness of the channels. The temperatures that prevail in the heat exchangers depend firstly on the temperature boundary conditions in the interior or the environment, secondly on the heat transfer coefficients u*A (W/K) and thirdly on the heat flow W. The heat flow is directly linked to the mass flow or mole flow of the H_2. Since the heat exchangers are not spatially resolved in the calculation, the air temperatures represent average values. The temperatures of R600a are assumed to be constant, as neither overheating nor subcooling can occur in this system.

Fig. 1 also shows the storage tank for the liquid refrigerant, which flows downwards after condensation and where it is collected in liquid form. The check valve prevents the pure H_2 gas at high pressure from flowing towards the condenser, which is at a lower overall pressure level. In order for the liquid refrigerant to enter the evaporator, the direction of operation of the H_2 compressor must be briefly reversed. This allows the liquid refrigerant to flow into the evaporator, where it is evenly absorbed into a fabric. There, the refrigerant

evaporates as the dry H_2 flows through it. As explained in the next section, the compressor operates with particularly high efficiency, so that a temperature of 15 °C above the condensation temperature is assumed for the compressed H_2 and the membrane. If the temperature is higher, an additional heat exchanger to the environment can be installed before the refrigerant enters the internal heat exchanger. Due to the high temperature of the membrane, the refrigerant condenses on the condenser wall that borders the environment.

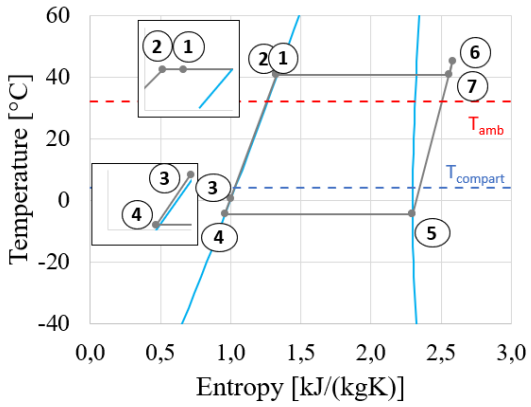

Figure 2. R600a Ts-diagram of the working process

Figure 2 shows the Ts-diagram of R600a with the conditions at the individual locations. The blue lines represent the saturation states. The locations are also marked with the same numbers in figure 1. This is shown for the operating case with a total pressure of 15 bar, an ambient temperature of 32°C, and a H_2 mass flow of 0.025 g/s. This corresponds to a cooling capacity of 20.7 W, which is assumed to be sufficient to maintain the temperature in the refrigerator. In state 1, the refrigerant has a total pressure of 14.94 bar and a condensation temperature of 40.6 °C. There is no H_2 at positions 1 to 3. The pressure difference to the pressure after the H_2-compressor is caused by flow losses, the calculation of which is explained below. State 2 with a pressure of 15 bar is achieved either by the discontinuous pumping process explained below or by a continuously operating pump arranged in place of the check valve. The rectangular section shows a zoom in of the two states (1 & 2) together with the blue line for the saturated liquid. State 3 is reached after flowing through the internal heat exchanger at a temperature of 0.5°C and a pressure of 14.97 bar. This corresponds to the assumption that the internal heat exchanger operates with a temperature difference of 5 K. Assuming that the same temperature prevails throughout the evaporator, an evaporation temperature of – 4.5°C is established. At this point, the pure H_2 in state 9 mixes with the R600a both at a temperature of 0.5°C. When thermodynamic equilibrium is reached, the evaporation temperature of -4.5°C is established in state 4 in the liquid R600a. The rectangular section again shows a zoom in of the two states (3 & 4) together with the blue line for the saturated liquid. At the evaporator outlet (state 5), the mixture exits with partial pressures of 13.64 bar (H_2) and 1.33 bar (R600a) and is heated to 49.8°C (state 6) in the internal heat exchanger. This is possible because the outlet temperature from the H_2 compressor is 15 K above the condensation temperature (state 8). In the condenser, the mixture is cooled to the condensation temperature of 40.6°C by heat transfer to the environment. Assuming that the same condensation temperature prevails throughout the condenser, partial pressures of 9.56 bar (H_2) and 5.38 bar (R600a) are established with a total pressure of 14.94 bar. All results are calculated with the following calculation model.

2.1. Calculation model

The calculation is based on the following assumptions. The calculation is performed for a time-stationary system. This is justified because the H_2 compressor can be operated continuously from standstill to a mass flow of 0.2 g/(m²s) in both directions. The power required for compression depends on boundary conditions such as temperature and pressure or pressure difference and other influences. In particular, with the large-area membranes assumed here, care must be taken to ensure an even flow so that the same temperatures and concentrations are present everywhere. The concentrations are decisive for the partial pressures and thus determine the pressure difference to the high-pressure side. The calculation assumes that these criteria are met. The power is calculated using the simple assumption of an isentropic change of state with the following equation:

$$P_s = \dot{m} \cdot \frac{\kappa}{\kappa-1} \cdot R \cdot T \cdot \left[\left(\frac{p_{hp}}{p_{pp}} \right)^{\frac{\kappa-1}{\kappa}} - 1 \right] \quad (1)$$

with:
- $\dot{m}$ — H_2 mass flow (kg/s)
- κ — isentropic coefficient (1,4)
- R — gas constant (J/kgK)
- T — temperature (K)

p_{hp}	H_2 pressure discharge side (Pa)
p_{pp}	H_2 partial pressure suction side (Pa)

To estimate the electrical power, an efficiency of $\eta_{el} = 0.9$ for the electrical control system is also taken into account:

$$P_{el} = P_s \cdot 1/\eta_{el} \tag{2}$$

*2.2. Considerations regarding the u*A values of the free convection heat exchangers*

When calculating heat transfer, it is assumed that the thermal resistance during condensation, evaporation and heat conduction in the wall is significantly lower than during free convection. Therefore, in a first approximation, the heat transfer coefficient is replaced by the heat transfer coefficient of free convection. Radiant heat exchange is not taken into account. The approach from the VDI Wärme-Atlas [12] is used to calculate the Nusselt number (Nu), which depends on the Rayleigh number (Ra) and the Prandtl number (Pr) as follows:

$$Nu = \left\{0.825 + 0{,}387 \cdot [Ra \cdot f_1(Pr)]^{1/6}\right\}^2 \tag{3}$$

with:

$$f_1(Pr) = \left[1 + \left(\frac{0.492}{Pr}\right)^{9/16}\right]^{-16/9} \tag{4}$$

and

$$Ra = \frac{g \cdot L^3 \cdot \beta \cdot (T_S - T_\infty)}{\nu \cdot \kappa} \tag{5}$$

with:	g	acceleration due to gravity (m/s²)
	L	vertical length (m)
	β	isobaric coefficient of expansion (1/K)
	κ	thermal conductivity (m²/s)
	ν	kinematic viscosity (m²/s)
	T_S	surface temperature (K)
	T_∞	ambient temperature (K)

The size and height of the surfaces play a decisive role in calculating the air-side heat transfer coefficients. Without an actual design being available, the maximum possible value is assumed for the external surfaces cooled by free convection. This assumes that all three vertical surfaces of the body with an area of 3 x 40 x 40 cm (# x H x W) can be used. This results in a total area of 0.48 m². For the evaporator, it is assumed that the maximum possible area with values of 3 x 40 x 30 (# x H x W) and thus 0.36 m² is also used. However, there is a reserve here, as the evaporator does not have to lie flush with the surface and therefore a downward flow would be created by the resulting cavity. However, this reserve was not taken into account in the calculation.

2.3. Estimation of flow cross-sections

Assuming a Newtonian fluid and a turbulent flow, the pressure loss (Δp) can be calculated using the following equation:

$$\Delta p = \frac{\rho}{2} \cdot c^2 \cdot \left(\frac{\lambda \cdot l}{d} + \zeta\right) \tag{6}$$

with:	ρ	density (kg/m³)
	c	fluid velocity (m/s)
	l	pipe length (m)
	d	pipe diameter (m)
	λ	pipe friction coefficient (-)
	ζ	pressure loss coefficient (-)

The volume ($\dot{V}$) flow can be estimated using the H_2 mass flow ($\dot{m}$), temperature (T), and pressure (p).

$$\dot{V} = \frac{\dot{m} \cdot R \cdot T}{p} \tag{7}$$

with:	$\dot{V}$	H_2 volume flow (m³/s)
	$\dot{m}$	H_2 mass flow (kg/s)
	R	gas constant (J/kgK)
	T	temperature (K)
	p	pressure (Pa)

With an average temperature of 286 K and a total pressure of 15 bar, a mass flow of 0.1 g/s of H_2 results in a volume flow of approx. 80 cm³/s. Assuming a flow velocity of 1 m/s, this results in a flow cross-section of 0.8 cm². These values produce a dynamic pressure of approx. 0.4 Pa. This means that the maximum pressure loss of 1 bar can be easily maintained without further consideration of pipe lengths or pressure loss coefficients.

2.4. H_2-compressor principle and characteristics

The functional principle and design schematics of an electrochemical H_2 compressor (EHC) single cell is given in Figure 3. H_2 at a pressure level pin is fed into the anodic side of an electrochemical cell, comparable to a battery, fuel cell or electrolyser. By passing through the flowfield and (micro-) porous gas diffusion layers (GDL and MPL), the molecules reach the surface of the catalyst coated membrane (CCM), where they are oxidised to form protons (H+) and electrons (e-). The protons are transported through the proton exchange membrane (PEM) and recombine with the electrons of the external circuit to reduce back to molecular hydrogen. The desired outlet pressure pout can be regulated via a back-pressure valve at the cell outlet. In order to achieve an efficient protonic transport, current membrane materials for low temperature applications (perfluorsulfonic-acid (PFSA) based Nafion®, or sulfonated poly(ether ether ketone) SPEEK), require a well-balanced hydration of the membrane with external H2O vapour supply. [13, 14]

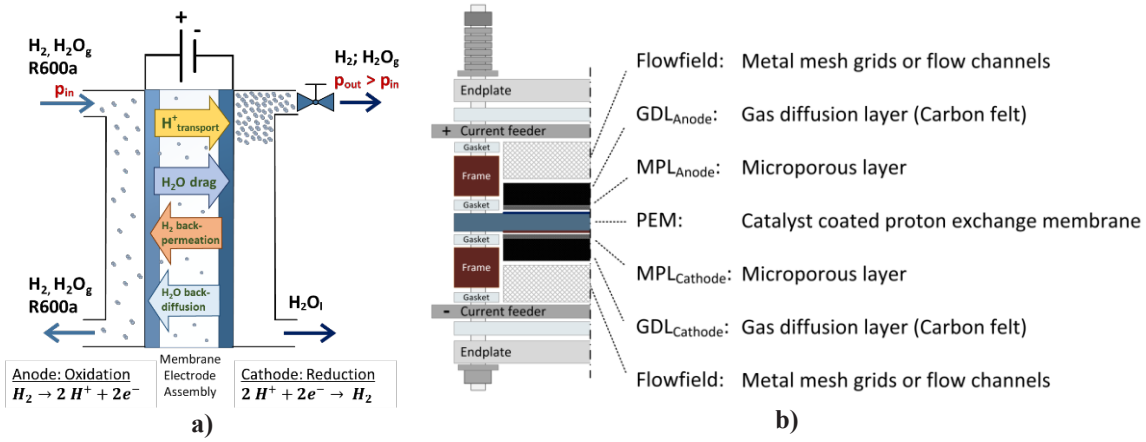

Figure 3: a) Principal schematic of electrochemical compressor with R600a, adapted from [15], b) layer-based design for single cell arrangement.

Apart from compressing pure H_2, the technology is further capable of extracting H_2 out of mixed media streams, with a clear focus on mixtures of natural gas (CH_4) and hydrogen. High H_2 yields of up to 90 % and low CH_4 impurity levels below 300 ppm were demonstrated [16]. To the best of the Author's knowledge, no study has been conducted separating R600a and H_2. However, as R600a has 3.6 times higher mol mass (58.12 g/mol) than methane (CH_4), the permeability of R600a through the membrane is assumed significantly lower than CH_4, while no negative effects of R600a on the catalysts (typically Pt/C) are expected. The technology is thus considered very promising for separating the two media flows, while experimental validation for permeability data of R600a through common membrane materials are recommended.

Assuming ideal gas behavior, the minimum required energy to realize the H_2 compression is given by the Gibbs free energy change (ΔG), with the Faraday constant (F) and the number of involved electrons (z) equal to 2.

$$\Delta G = \Delta G^0 + R \cdot T \cdot \ln\left(\frac{p_{H_2}^{out}}{p_{H_2}^{in}}\right) = -z \cdot F \cdot E \tag{8}$$

The standard Gibbs free energy of H_2 formation (ΔG^0) is equal to 0, leading to the simplified Nernst equation with a minimum required cell voltage E_N (Nernst voltage).

$$E_N = \frac{R \cdot T}{z \cdot F} \ln\left(\frac{p_{H_2}^{out}}{p_{H_2}^{in}}\right) \tag{9}$$

For a partial pressure ratio $p_{H2,out}/p_{H2,in}$ of 13.3 (8 to 0.6 bar), according to the pressure ratios of the refrigeration system described above, and a cell temperature of T = 50 °C, a theoretical Nernst voltage of E_N equal to 36 mV is required. However, the actual cell voltage (E_{cell}) in operation is determined by several overpotentials associated with specific losses due to activation of the catalyst (η_{act}), ohmic resistances of the protonic transport and electrical contact (η_{ohmic}), and mass-transport resistances within the several cell layers ($\eta_{mass\text{-}transfer}$) [14]. The theoretical H_2 mass flow through the membrane $(\dot{m}_{H_{2,F}})$ is given by Faraday's law, with the current density i, the active cell area A and the mol mass M (Figure 4).

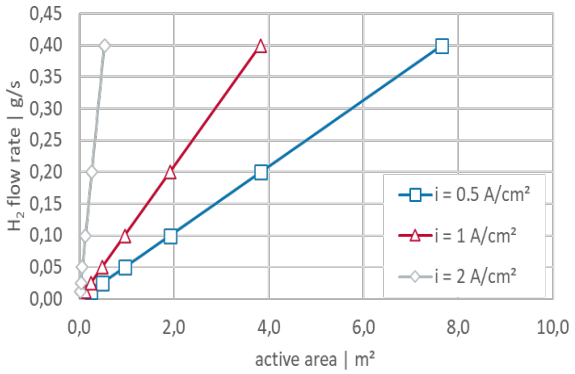

Figure 4: Theoretical flow rates of H_2 based on Faraday's law as function of the operating current density i

As the resulting H_2 flow is a function of the operating current, it can be adjusted according to the current refrigeration requirements. Depending on the actual H_2 partial pressure ratio, a certain amount of H_2 is permeating back from the high-pressure side to the low-pressure side which reduces the H_2 yield. The back-permeation increases significantly with increasing temperature and pressure ratio, but can be limited applying thicker membranes. In contrast, thicker membranes result in higher ohmic resistances, possible humidification issues and generally lower voltage efficiency. Therefore, selecting a membrane thickness suitable for the application is one of the most important design criteria for an efficient compression process [15]. The overall efficiency of the electrochemical membrane compressor (η_{EHC}) is given by multiplying the voltage efficiency (η_E) with the Faraday efficiency (η_F), describing the hydrogen yield

$$\eta_{EHC} = \eta_E \cdot \eta_F = \frac{E_{cell}}{E_N} \cdot \frac{\dot{n}_{H_{2,F}} - \dot{n}_{H_2,perm}}{\dot{n}_{H_{2,F}}} \tag{10}$$

With thin membranes of 30 µm (Nafion® XL), overall efficiencies of 53% were reached for pressure ratios of 32 and operating current densities of 0.66 A/cm². At low current densities below 0.5 A/cm² and moderate pressure ratios of 10-20 as required in the refrigeration application, efficiencies of over 60 % are currently feasible, with theory [17]. Attaining high flow rates demands either large membrane areas or high current densities, which must be balanced against efficiency losses and system costs. Detailed cost data is publicly not available, but high material costs of the membrane electrode assembly and gas diffusion layers emphasise the importance of reducing the system size at given flow rates. [18] Sdanghi et al. projected specific system costs of 1700 $/(kg/d) for pressure ratios below 100. [19]
Due to its flat design (compare Figure 3 b), based on multiple planar layers (end plates, current collectors, media flow fields, gas diffusion layers, catalyst coated membrane), a single cell compressor arrangement with a vertical dimension of 1 to 2 cm is feasible. The core components comprising the catalyst coated membrane and gas diffusion layers including the microporous layers sum up to a height of about 600 µm. Finally the membrane size of approx. 0,48 m² together with a current density i = 0,5 A/cm² would result in H_2 mass flow of 0.024 g/s at an efficiency of over 60%. This would provide a cooling capacity of approx. 20 W for a total pressure of 15 bar (see figures 5 and 6).

2.5. Calculation results

The numerical solution of the equations is performed in Excel, taking into account the material values and the conservation equations for energy and mass. The process is repeated until the smallest temperature change from iteration to iteration is less than 0.001 (K).

The calculation is performed in Excel for the following input values:

Table 1. Calculated boundary conditions for the compartment temperature T_{Comp} = 4 °C

	Lower value	Higher Value
Ambient temperatures	25 °C	32 °C
Discharge pressure compressor	8 bar	20 bar
H_2 mass flow	0,005 g/s	0,1 g/s

2.6. Calculation results

The calculations were performed for increasing H_2 mass flows and ambient temperatures of 25 °C and 32 °C. In addition, the effect of a total pressure variation between 8 bar to 20 bar for a cooling capacity of 50 W was also calculated.

Diagram 1 shows the results for a variation in H_2 mass flows between 0 and 0.1 g/s. Total pressure is 15 bar and ambient temperature is 25 °C. The selection of H_2 mass flows is based on the cooling capacity achieved, which reaches a value of 53.8 W for 0.1 g/s. The cooling capacity cannot follow the linear increase in H_2 mass flow but behaves degressively. The reason for this lies in the increasing temperature differences at the condenser and evaporator, with values of 18.9 (K) (condenser) and -17.6 (K) (evaporator) for the cooling capacity of 53.8 W. Similarly, the COP falls from the theoretical value of 3.16 at minimum cooling capacity to 0.560 at 53.8 W. An ambient temperature of T_a = 32°C worsens the COP values, but the other curves remain almost the same. Both the temperature differences at the condenser and evaporator and the cooling capacity curve remain unchanged compared to the case with an ambient temperature of T_a = 25°C. This can be explained by the fact that the mass flow of R600a depends only on the H_2 mass flow and the evaporation pressure. The cooling capacity, in turn, depends only on the mass flow of R600a. The higher compressor capacity required for an increased ambient temperature T_a, results from the higher saturation pressure of R600a at 32 °C compared to 25 °C.

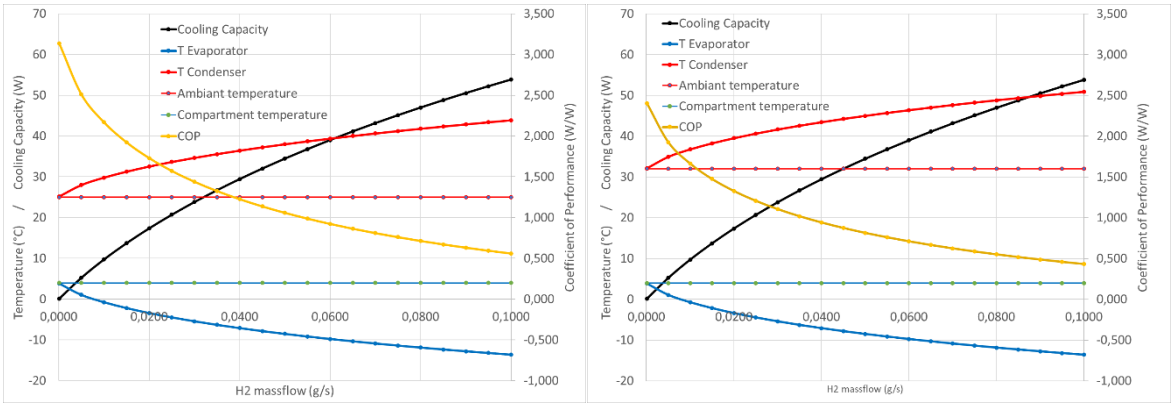

Figures 5, 6. Calculation results for the variation of H_2 mass flow, ambient temperatures T_a = 25°C (left side) and T_a = 32°C (right side)

The influence of the total pressure is examined as a further influencing factor. In extreme cases, the partial pressure of R600a in the condenser may correspond to the condensation pressure. However, this means that the partial pressure of H_2 approaches zero, resulting in an extreme pressure ratio for the compressor. If the total pressure is lower than the condensation pressure of R600a, the system will not function. For this reason, the total pressure was varied in 2 bar increments between 8 bar and 20 bar for an ambient temperature of T_a = 32 °C and a cooling capacity of 50 W. Figure 7 shows a constant evaporation temperature, which corresponds to the constant cooling capacity. However, the condensation temperature shows a slight upward trend, which is related to the higher H_2 mass flow. The strongest correlation to the total pressure, however, is with the required H_2 mass flow, which reaches a value of 0.0394 g/s at a total pressure of 8 bar and a value of 0.1393 g/s at a total pressure of 20 bar. The COP curve shows a maximum at a total pressure of 16 bar with a value of 0.475 and an H_2 mass flow of 0.09 g/s.

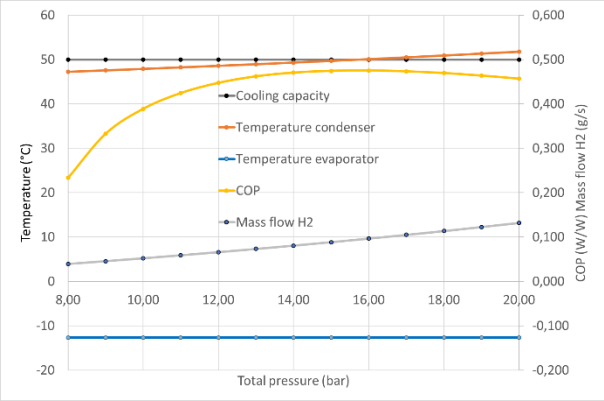

Figure 7. Calculation results for the variation of total pressure for a cooling capacity of 50 W.

2.7. Stand-by efficiency

However, standby energy consumption is decisive for assessing energy efficiency. Here, the quality of the appliance's insulation determines the continuous heat input. The use of a glass door is a major disadvantage, as even triple glazing does not achieve a heat transfer coefficient of less than 0.5 (W/m²K). In comparison, today's freezers achieve values of 0.2 (W/m²K). This value together with a surface area of 1.12 (m²) with the assumed geometry (40 x 40 x 50 cm) would result in a heat input value of 4.7 W at an ambient temperature of 25 °C. For poorly insulated appliances, a heat input value of 10 W is quite possible just to maintain the temperature. The proposed system clearly has advantages here, as it can generate cooling capacity from 0 to 50 W continuously. In contrast, a classic vapor compression refrigeration system can only achieve these low capacities through intermittent operation. As can be seen from figures 5 and 6, the COP increases significantly for low cooling capacities. For a heat input of approx. 5 W, the system achieves values of 2.5. The low performance figures resulting from high cooling capacities are mainly due to the low heat transfer coefficients that occur during free convection. Free convection, combined with the small vertical dimensions and small surfaces, is a key reason for the low energy efficiency of these devices, even with any other refrigeration system.

2.8. Advantages and disadvantages of the system

- When correctly designed, the system operates extremely quietly. Only the flow noise remains, which is negligible at low speeds.
- The proposed system can generate cooling capacity from 0 to 50 W continuously for the proposed device geometry. In contrast, a conventional vapor compression refrigeration system can only achieve these low capacities through intermittent operation. As can be seen from diagrams 1 and 2, the coefficient of performance increases significantly for low cooling capacities. For a heat input of approx. 5 W, the system achieves values of 2.5.
- The refrigeration system consists mainly of vertical surfaces that form a layered structure and can therefore be used directly as a wall.
- Current research at HyCentA also includes membrane compressors that can extract H_2 in high purity from gas mixtures. Research on the H_2 compressor is moving towards lower water consumption and more cost-effective membrane materials.
- However, the H_2-compressor also needs water at the membrane to function, which can be in the form of water vapor or liquid water. First an initial hydration of the membrane is needed. Later during the compression process water molecules are transferred from the anodic side to the cathodic side as a result of the electrostatic draw between protons and water molecules. This electroosmotic drag amounts to approximately 9 g H_2O per g of H_2 (1.8 mol H_2O per mol H_2). Consequently, a well distributed humidification of the membrane is required for an effective protonic transport.
- In addition to the lack of experience with systems that have actually been implemented, there are other arguments against their imminent use.
- The use of H_2 as a transport gas poses a fire hazard in the event of an accidental leak. Assuming that the total volume is equal to the surface area of the condenser and evaporator multiplied by a thickness of 1 cm, this results in a volume of approx. 8.4 dm³. At a pressure of 20 bar and an average temperature in both heat exchangers of 13°C, this results in an H_2 mass of approx. 14 g.
- The membrane is expensive and consists of a Teflon-like material that will most likely fall under the EU's PFAS Directive [(EU) 2019/1021] in the future.
- The transport of H_2 through the membrane requires a certain amount of water vapor. This would be transported as contamination from the discharge side of the H_2 compressor towards the internal heat exchanger, where it would freeze. Although the flow direction of the compressor can be easily reversed, thereby probably also thawing the ice that has formed, the handling of three substances is

complex. This results in the need for a cost-effective membrane that does not require additional aids or hazardous substances.
The condensed refrigerant R600a must be returned to the evaporator against the rising total pressure. As shown in the explanation for Figure 2, the total pressure in the condenser is lower than in the evaporator. As can be seen from the example, the pressure difference is small, at approx. 0.03 bar. One option is to use a pump to create a continuously operating process. Due to the requirement that there should be no mechanical drive and therefore no conventional pump, the following process can also be used as an alternative. The electrical polarity reversal also reverses the direction of flow through the compressor. This briefly increases the pressure in the condenser and decreases it in the evaporator, pumping the liquid refrigerant from the reservoir (1) via the check valve into the internal heat exchanger and finally the evaporator (4), where it wets the sponge-like structure. Immediately afterwards, the regular cooling process begins again. Thermodynamic effects were not taken into account in the calculation.

3. Conclusion

This paper presents a refrigeration process that can absorb heat at low temperatures via the evaporation of the refrigerant R600a. Due to the presence of a second gas, in this case H_2, the two partial pressures add up to a total pressure that only decreases due to flow losses in the direction of flow. Since the H_2 compressor after the condenser separates the two gases perfectly on the one hand and brings the H_2 to a higher pressure on the other, the refrigerant accumulates in the condenser. This increases the partial pressure of the refrigerant and it condenses when the saturation pressure is exceeded. The condensation heat released in the process is transferred to the environment and the liquid phase flows downwards, where it is collected in a collection tank. Finally, the liquid refrigerant is returned to the evaporator and the cycle begins again.

To evaluate the efficiency of the system, a model for the virtual geometry of a minbar refrigerator was created, taking into account the basic conservation equations and the thermophysical properties. The calculations for the variation in the H_2 mass flow show that, for low cooling capacities of 5 to 10 W, depending on the ambient temperature, high COP values of over 2 can be achieved. For high cooling capacities in the range of 50 W, the COP values are much lower. This is not only due to the assumed flow pressure losses of 1 bar, but rather to the low heat transfer coefficients for free convection in the range of 5 W/m²K due to the small vertical dimensions. This results in temperature differences of 15 to 18 K in order to transfer the heat output.

The H_2 compressor, which is an important component in the proposed cooling process, has several major disadvantages. The membrane can only transport or compress H_2 with a third substance namely water (H_2O). This means that the water must also be transported to the right places in the cycle without freezing which is a complex task. In future, the membranes will be subject to the EU's PFAS Directive, making it unlikely that they will be permitted for use in areas where alternative processes are available. The price of the membranes is currently very high. Current research is therefore focusing on alternative membrane technologies.

Acknowledgements

This scientific paper was significantly supported by the COMET project ECHODA. ECHODA is funded within the framework of COMET - Competence Centers for Excellent Technologies by BMWET, BMIMI, the province of Styria as well as SFG. The COMET programme is managed by FFG.

The H_2-research was carried out within the HyCentA COMET Centre (grant ID 892427). The COMET Centre HyCentA is funded within COMET – Competence Centers for Excellent Technologies – by BMK, BMAW as well as the cofinancing federal provinces Styria, Upper Austria, Tyrol and Vienna. The COMET programme is managed by FFG.

References

[1] Verified Market Reports, 2025. Global Hotel Refrigerator Market Size, https://www.verifiedmarketreports.com/de/product/hotel-refrigerator-market/:, retrieved on 12_Jan_2026

[2] Najjarana, A., Freemana, J., Ramosa, A., Markidesa, Ch. N., 2019. Experimental investigation of an ammonia-water-hydrogen diffusion absorption refrigerator. Applied Energy, No 256, 113899.

[3] Zohar, A., Jelinek, M., Levy, A., Borde, I., 2003. An experimental investigation of bubble pump performance for diffusion absorption refrigeration systems with organic working fluids. Applied Thermal Engineering 23, 1881-1894.
[4] Taieb, A., Mejbri, K., Bellagi, A., 2016. Detailed thermodynamic analysis of a diffusion-absorption refrigeration cycle. Energy 115, 418-434.
[5] Chavan, P., Kaur Sidhu, G., 2021. Performance Evaluation of Mobile Liquid Cooled Thermoelectric Refrigeration System for Storage-cum-Transportation of Fruits and Vegetables. Research Square, DOI: https://doi.org/10.21203/rs.3.rs-543847/v1
[6] EC Directorate-General for Energy: European Eprel database, 2025 EPREL - 1.0.101 - 22/10/2025, https://eprel.ec.europa.eu/screen/home
[7] Kim, J., Mishra, A., Braun, J. E., Groll, E. A., Rodriguez-Lopez, J., Ziviani, D., 2023. Electrochemically driven phase transformation for high-efficiency heat pumping. Cell Reports Physical Science 4, 101369, https://doi.org/10.1016/j.xcrp.2023.101369
[8] James, N. A., Braun, J. E., Groll, E. A., Horton, W. T., 2016. Thermodynamic Analysis of an Electrochemically Driven Chemical Looping Heat Pump. International Refrigeration and Air Conditioning Conference. Paper 1745. https://docs.lib.purdue.edu/iracc/1745/
[9] Liebl, L., Bardow, A., Roskosch, D.,2024. Indirect Electrochemical Cooling: Model-Based Performance Analysis and Working Fluid Selection, Ind. Eng. Chem. Res. 2024, 63, 1055−1065 https://doi.org/10.1021/acs.iecr.3c03582
[10] NIST Refprop, REFPROP v10.0, 2022.
[11] Brown, J. St., Domanski, P. A., 2014. Review of alternative cooling technologies. Applied Thermal Engineering, 64, 252-262.
[12] Stephan, P., Kabelac, St., Kind, K., Mewes, D., Schaber, K., Wetzel, Th., 2019. VDI-Wärmeatlas, F2 Wärmeübertragung durch freie Konvektion: Außenströmung, 763-773
[13] Durmus, G., Colpan, C., Devrim, Y., 2021. A review on the development of the electrochemical hydrogen compressors. Journal of Power Sources, Nr. 494, p. 229743.
[14] Marcius, D., Kovac, A., Firak, M., 2022. Electrochemical hydrogen compressor: Recent progress and challenges. International Journal of Hydrogen Energy, Nr. 47, pp. 24179-24193.
[15] Richter, M., Keuschnigg, C., Grabner, B., Macherhammer, M.-G., Trattner, A., 2025. Investigation of favourable operating conditions for electrochemical hydrogen compressors by 3D CFD simulation and single cell tests. International Journal of Hydrogen Energy, Nr. 185, p. 150251.
[16] Mrusek, S., Blasius, M., Morgenroth, F. , Thiele, S., Wasserscheid, P., 2023. Hydrogen extraction from methane-hydrogen mixtures from the natural gas grid by means of electrochemical hydrogen separation and compression. International Journal of Hydrogen Energy, Nr. 50, pp. 526-538.
[17] Sdanghi, G., Dillet, J., Didierjean, S., Fierro, V., Maranzana, G., 2019. Feasibility of hydrogen compression in an electrochemical system: Focus on water transport mechanisms. Fuel Cells, Nr. 20, pp. 370-380.
[18] Parida, A., Muthukumar, P., Dalal, A., 2025. A review on non-mechanical hydrogen compressors for hydrogen refuelling stations. International Journal of Hydrogen Energy, Nr. 145, pp. 292-321.
[19] Sdanghi, G., Maranzana, G., Celzard, A., Fierro, F., 2019. Review of the current technologies and performances of hydrogen compression for stationary and automotive applications. Renewable Sustainable Energy Reviews, Nr. 102, pp. 150-170, 2019.